JVI Journals.ASM.org

Crystal Structure of the Japanese Encephalitis Virus Envelope Protein

Vincent C. Luca,[a,b] Jad AbiMansour,[a] Christopher A. Nelson,[a] and Daved H. Fremont[a,b]

Department of Pathology and Immunology[a] and Program in Molecular Biophysics,[b] Washington University School of Medicine, St. Louis, Missouri, USA

Japanese encephalitis virus (JEV) is the leading global cause of viral encephalitis. The JEV envelope protein (E) facilitates cellular attachment and membrane fusion and is the primary target of neutralizing antibodies. We have determined the 2.1-Å resolution crystal structure of the JEV E ectodomain refolded from bacterial inclusion bodies. The E protein possesses the three domains characteristic of flavivirus envelopes and epitope mapping of neutralizing antibodies onto the structure reveals determinants that correspond to the domain I lateral ridge, fusion loop, domain III lateral ridge, and domain I-II hinge. While monomeric in solution, JEV E assembles as an antiparallel dimer in the crystal lattice organized in a highly similar fashion as seen in cryo-electron microscopy models of mature flavivirus virions. The dimer interface, however, is remarkably small and lacks many of the domain II contacts observed in other flavivirus E homodimers. In addition, uniquely conserved histidines within the JEV serocomplex suggest that pH-mediated structural transitions may be aided by lateral interactions outside the dimer interface in the icosahedral virion. Our results suggest that variation in dimer structure and stability may significantly influence the assembly, receptor interaction, and uncoating of virions.

Japanese encephalitis virus (JEV) is the leading cause of viral encephalitis worldwide; it is responsible for 30,000 to 50,000 cases and 10,000 deaths annually in eastern Asia. The virus is arthropod-borne and naturally cycles between mosquitoes and pigs or wild birds but may also be transmitted to humans and horses (29). There are multiple vaccines for JEV, but they are not universally available in Asia due to cost, licensing issues, and safety concerns (45, 51, 55, 60). JEV is a member of the *Flavivirus* genus, along with several other viruses, including West Nile virus (WNV), tick-borne encephalitis virus (TBEV), and dengue virus (DV).

Flaviviruses are positive-stranded RNA viruses with a 9- to 12-kb genome that is translated as a single polyprotein that is cleaved by host and viral proteases into structural capsid (C), premembrane (prM), and envelope (E) proteins and seven nonstructural proteins. Capsid binds to viral RNA and forms a nucleocapsid that is enveloped by an endoplasmic reticulum-derived membrane containing E and prM. E proteins are responsible for cellular attachment and possess a hydrophobic loop that mediates fusion of viral and host membranes (3, 8, 11, 21, 32, 42).

During its life cycle, the JEV virion undergoes a maturation process that continuously shields the fusion peptide from premature insertion into the host cell membrane. In an immature virion, E forms irregular trimers with fusion loops capped by prM until it is cleaved in the *trans*-Golgi network prior to viral secretion (15, 57, 64). E then rearranges into an icosahedral network of flat antiparallel homodimers that bury the loop at their interface (31, 52). Mature virions attach to cells and are taken up into the endosome where the acidic environment triggers an irreversible change from dimer to trimeric spikes (2, 5, 37, 43). This process exposes the fusion loops that penetrate the endosome and drags together host and viral membranes, thereby releasing the nucleocapsid into the cell.

The majority of flavivirus neutralizing antibodies bind E and can inhibit several stages of the entry process, including attachment and fusion (20, 46, 48, 49, 61, 63). Infection with a flavivirus results in the generation of broadly cross-reactive antibodies, but the polysera from a given infection will only neutralize a subset of other viruses. This phenomenon is the basis for the serocomplex system of classification in which flaviviruses are placed into groups defined by cross-neutralization tests with polysera from heterologous infections (12). Clinical manifestations of infection are retained within a given serocomplex and range from febrile illness to hemorrhagic fever. The JEV serocomplex includes St. Louis encephalitis virus (SLEV), WNV, and prototypical member JEV, all of which are known to cause flu-like symptoms and acute or fatal encephalitis (12, 56). The remaining serocomplexes also exhibit specific tropisms and pathogeneses, the most notable of which are represented by TBEV, yellow fever virus, and DV.

We have determined here the crystal structure of the JEV E protein to investigate whether structural features could contribute to our understanding of serocomplex-specific pathogenesis. The E protein crystallized as the canonical head-to-tail flavivirus E protein dimer but with a notably small interface. The JEV E dimer has roughly half the buried surface area of any known flavivirus E structure, and the majority of its contacts are between the fusion loop and domain I (DI)-DIII pocket, not at the central dimerization region. We suggest that this smaller dimer interface may be the preferred organization of E proteins from viruses in the JEV serocomplex and that it provides an effective atomic model for JEV E within mature virions.

MATERIALS AND METHODS

Cloning, expression, and purification of soluble JEV E, SLEV E, and WNV E. A cDNA encoding ectodomain residues 1 to 406 of the JEV E from the SA-14-14-2 strain protein and those of WNV and SLEV E was cloned into the bacterial expression vector pET21a(+). This vector was transformed into BL21(DE3) (RIL) cells (Stratagene), grown in a large-scale 4-liter culture, and induced at an optical density at 400 nm of 0.8 with 1 mM IPTG (isopropyl-β-D-thiogalactopyranoside). After 4 h, the cells were centrifuged, and pellets were suspended in 50 ml of solution

Received 19 August 2011 Accepted 22 November 2011
Published ahead of print 7 December 2011
Address correspondence to Daved H. Fremont, fremont@wustl.edu.

doi:10.1128/JVI.06072-11

buffer (50 mM Tris [pH 8.0], 25% sucrose, 10 mM dithiothreitol [DTT]), and then an equal amount of lysis buffer (50 mM Tris [pH 8.0], 1% Triton X-100, 100 mM NaCl, 10 mM DTT) was added. The mixture was treated with 0.8 mg of lysozyme/ml and sonicated three times for 15 s to disrupt cell membranes. Next, the lysate was centrifuged at 10,000 × *g*, and the pellet containing the protein inclusion bodies was washed three times with 50 ml of wash buffer (50 mM Tris [pH 8.0], 0.5% Triton X-100, 100 mM NaCl, 1 mM DTT) and then once in wash buffer without Triton X-100. Purified inclusion body pellets were resuspended in 20 ml of TE buffer (10 mM Tris [pH 8.0], 1 mM EDTA), and 2-ml aliquots of this slurry were each solubilized in 10 ml of 6 M guanidine-HCl, 10 mM Tris (pH 8.0), and 20 mM β-mercaptoethanol. These aliquots were rapidly diluted by adding 1 ml every 30 min dropwise into a rapidly stirring 1-liter reservoir of oxidative refolding buffer (400 mM nondetergent sulfobetaine-201, 100 mM Tris [pH 8.0], 0.5 mM oxidized glutathione, 5 mM reduced glutathione) for overnight refolding. The refolded protein was concentrated to a volume of 10 ml using an Amicon 400 concentrator with 30-kDa cutoff membrane and purified on a S200 size exclusion chromatography (SEC) column. Protein was isolated from eluted fractions corresponding to a predicted molecular mass of 20 kDa, suggesting that it interacts with the Sephadex beads of the column since the purified protein was full length. This material was further purified on a Mono-Q anion-exchange column.

Expression and purification of DV2 E. Residues 1 to 394 of DV2 E ectodomain with an N-terminal honeybee melittin signal sequence were cloned into the baculovirus transfer vector pAcUW51. The DV2 E encoding transfer vector was then cotransfected into SF9 cells grown in serum-free Sf-900 II medium (Invitrogen) with the Flashbac Gold bacmid (Oxford Expression Technologies) to allow homologous recombination to generate recombinant baculoviruses. The virus was then amplified by passaging the supernatant at ratios of 1:10 into fresh SF9 cultures until the titer was sufficient for large-scale expression. A total of 5 liters of Hi-Five cells grown in Express Five (Invitrogen) serum-free medium were then infected with recombinant virus to drive expression of secreted DV2 E. The supernatant from the large-scale infection was then filtered with a 0.2-μm-pore-size cutoff bottle-top filter, concentrated, and buffer exchanged into nickel binding buffer (300 mM sodium citrate, 150 mM NaCl, 50 mM $NaPO_4$ [pH 8.0]) using a Cetramate tangential flow concentrator with 30-kDa cutoff membrane. This supernatant was then purified by nickel and size exclusion chromatography.

Crystallization of JEV E. Soluble JEV E protein was crystallized at 20°C by hanging drop vapor diffusion. Drops containing 0.5 μl of protein at a concentration of 10 mg/ml were combined with 0.5 μl of mother liquor containing 0.1 M Tris (pH 8.0), 16% polyethylene glycol (PEG) 3350, and 0.2 M sodium citrate, and diffraction-quality crystals grew in 3 days. The crystals were cryoprotected by transferring them briefly into a drop containing 10% PEG 3350, 25% glycerol, 0.2 M sodium citrate, and 0.1 M Tris (pH 8.0) and then cooling them in liquid nitrogen. The data were collected with the Advanced Photon Source beamline 21-ID-F. The data set was processed, integrated, scaled, and merged using HKL2000 (36). JEV E crystallized in space group I222 with unit cell dimensions of $a = 61.1$ Å, $b = 62.4$ Å, and $c = 243.0$ Å and contains one molecule per asymmetric unit.

Structure determination. The structure of JEV E was solved using molecular replacement. The WNV E protein (PDB ID 2HG0/2I69) was used as a model in Phaser via the PHENIX graphical user interface (1). Mutation of amino acid side chains and model building was done in Coot (27). The model was refined to a 2.1-Å resolution in several steps using PHENIX. Initially, rigid body refinement of each of the three domains was performed, followed by atomic refinement and automated addition of waters. Coordinates were then uploaded to the TLSID server to obtain domain predictions for translation liberation screw refinement (35, 50). The resultant structure has a final R_{work} of 18.0%, an R_{free} of 22.1%, and a total of 214 waters. The N-terminal 403 of 406 amino acids of the E protein construct were built into the model.

TABLE 1 X-ray data collection and refinement statistics for the JEV E protein ectodomain

Parameter	Value(s)[a]
Data collection	
Space group	I222
Cell dimensions (*a*, *b*, *c* [Å])	61.11, 62.40, 243.04
Resolution (Å) (high-resolution shell)	50.0–2.10 (2.18–2.10)
Completeness (%)	99.24 (99.8)
Redundancy	4.3 (4.4)
I/σ	12.1 (2.0)
R_{merge} (I)	0.07 (0.427)
Refinement	
Resolution range (high-resolution shell)	30.2–2.10 Å (2.17–2.10 Å)
R_{work} reflections[b] ($F > 0$)	25,663 (2,470)
R_{free} reflections	1,284 (136)
R_{work}	0.1811 (0.2037)
R_{free}	0.2242 (0.2294)
JEV E residues (no. of atoms)	403 (3,045)
No. of solvent atoms	210
Estimated coordinate error	0.230
Wilson B-factor (Å^2)	27.62
RMSD bond length (Å)	0.009
RMSD bond angle (°)	1.098

[a] Values in parentheses are for data in the highest-resolution shell.
[b] Statistics as defined in PHENIX.

Multi-angle light scattering. JEV, WNV, SLEV, and DV2 E proteins (200 μg) were loaded in sizing buffer (150 mM sodium chloride, 20 mM HEPES [pH 7.4], 0.01% sodium azide) onto a size exclusion chromatography column set up in series with a Dawn Helios II multi-angle light scattering detector (Wyatt), Optilab rEX (Wyatt) differential refractive index detector, and photodiode array detector 996 (Waters). The light scattering, refractive index change, and UV absorbance were each observed over the elution profile. The data were then analyzed with the Astra V macromolecular characterization software package (Wyatt) to calculate the molecular mass of each protein from the light scattering and refractive index change.

Protein structure accession number. The coordinates for JEV E have been deposited in the RCSB Protein Data Bank (PDB accession code 3P54).

RESULTS

Bacterial expression and refolding of JEV E protein. Recombinant JEV E protein spanning residues 1 to 406 of the ectodomain was produced in *Escherichia coli* as inclusion bodies and refolded by methods previously described for WNV E (7). Briefly, inclusion bodies were solubilized in guanidine-HCl and β-mercaptoethanol and refolded by dilution into a buffer containing a 10:1 ratio of reduced to oxidized glutathione to allow for proper formation of disulfide bonds. Soluble E was then purified by size-exclusion chromatography and anion-exchange chromatography. Envelope proteins from JEV, WNV, and SLEV were purified by this method, proving its effectiveness as a low-cost alternative for the production of recombinant flavivirus E proteins.

Structure of JEV E protein. Crystals of the JEV ectodomain diffracted to 2.1 Å, and the structure was solved with an R_{work} of 22% and an R_{free} of 18% (data collection and refinement statistics are presented in Table 1). While refolded from bacterial inclusion bodies, JEV E retained the three-domain organization and disulfide connectivity previously observed in other flavivirus E proteins (Fig. 1) (23, 38, 39, 47, 52, 65). The central domain I (DI) is

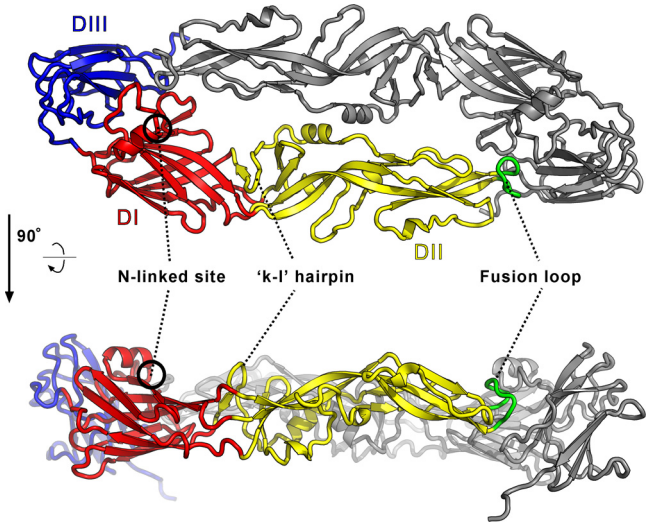

FIG 1 Crystal structure of JEV E ectodomain. JEV E possesses the three domains characteristic of flavivirus E with symmetry operators that allow for generation of the canonical E dimer. A JEV E diagram representation crystal structure is shown, with domain I highlighted in red, domain II highlighted in yellow, domain III highlighted in blue, and the crystallographic dimer generated from orthorhombic symmetry highlighted in gray. The structure is also shown rotated 90° into the page. The fusion loop is colored green, and the "k-l" loop and glycosylation site are indicated in both structures.

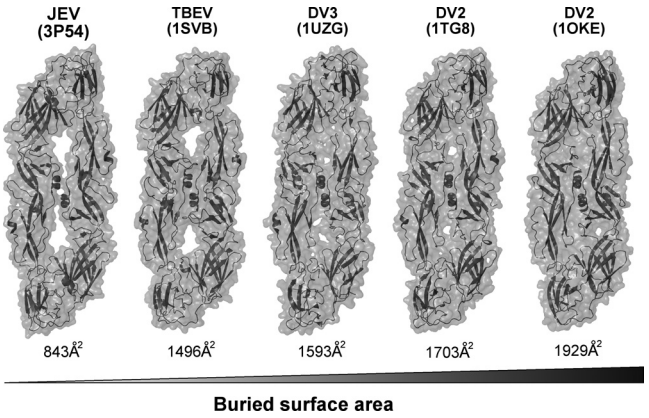

FIG 2 Relative buried surface area of dimeric flavivirus E protein structures. JEV E has a small dimer interface relative to other E crystal structures. Surface representations of known dimeric E protein crystal structures are displayed arranged in ascending order of buried surface area. Note that JEV E and TBEV E have visible solvent channels between subunits at the dimer interface, features that are absent in DV E dimers that have greater contact interfaces.

composed of a nine-stranded β-barrel located between the extended domain II (DII) and the globular domain III (DIII). DII is formed out of two extended loops that protrude from DI, the larger of which is stabilized by three disulfide bonds and contains the conserved fusion peptide at its tip. DIII possesses an immunoglobulin-like fold and is found at the C terminus of the ectodomain, connected to DI by a short peptide linker. The crystals only contained one molecule in the asymmetric unit, but application of the orthorhombic symmetry operators allowed for the generation of the archetypal flavivirus envelope dimer.

N-linked glycosylation site. The location and presentation of the glycan linked to N^{154} has been linked to particle infectivity and interaction with putative cellular receptors DC-SIGN or DC-SIGNR (10, 11, 18). Recombinant JEV E ectodomain was purified from bacterial inclusion bodies by oxidative refolding and therefore lacks this modification. In order to evaluate whether the E_o-F_0 loop region of JEV E is affected by glycosylation at N^{154}, it was superimposed onto the glycosylated loop of the closely related WNV E structure. The main chain traces in this region overlay residues 144 to 164 with an overall root mean square deviation (RMSD) of only 0.45, suggesting that glycosylation does not significantly affect the presentation of this region.

Dimer interface. The most unusual feature of the JEV E structure is its curiously small dimer interface. On the surface of the mature virion, flavivirus E proteins exist as an antiparallel dimer with the fusion peptide of DII nestled into a cavity formed by DI and DIII on the opposing subunit (31). In the DV and TBEV E structures, there are extensive contacts across the DII-DII interface that stabilize this assembly. Several properties of the dimer from JEV, DV2, DV3, and TBEV envelope proteins were analyzed using the PISA (protein interfaces, surfaces and assemblies) server (Table 2) (30). Although the secondary and tertiary structure of JEV E is similar to those of other E proteins, it has only 44 to 56% of the buried surface area observed in other flavivirus E dimers (Fig. 2). In addition, it is not stabilized by any salt bridges and has far fewer hydrogen bonds across the assembly. The JEV E dimer has 843 Å^2 of total buried surface area, whereas the lowest total buried surface area of any other structure is TBEV E with 1,496 Å^2. Further analysis revealed that the largest disparity lies at the DII-DII interface. At this site JEV E only has 150 Å^2 buried surface area, compared to 534 Å^2 or greater for all of the other E proteins. The DI-DIII pocket that houses the fusion loop has relatively less buried surface area as well, but the difference at this surface is at most 0.4-fold, compared to >3-fold for the DII-DII interface. These values reinforce the conclusion that DII-DII contacts are deficient in the JEV dimer. The surface complementarity (S_c) across domain II of JEV E was only 0.372, a value below what is believed to signify a relevant protein-protein interaction. The other E proteins were found to have an S_c of >0.6, in line with other biolog-

TABLE 2 Analysis of E protein dimer interfaces

Envelope	BSA (Å^2)			S_C			No. of:		
	Total	D13-D2	D2-D2	Total	D13-D2	D2-D2	Interface residues	H bonds	Salt bridges
JEV (3P54)	843.1	346.8	149.4	0.786	0.799	0.372	38	2	0
DV2-βOG (1OKE)	1,929.2	577.5	825.2	0.719	0.766	0.655	62	17	4
DV2 (1TG8)	1,703.0	557.5	613.9	0.735	0.790	0.612	57	20	5
DV3 (1UZG)	1,593.2	533.6	534.6	0.654	0.629	0.602	51	12	2
TBE (1SVB)	1,496.2	412.8	672.1	0.702	0.754	0.633	49	8	2

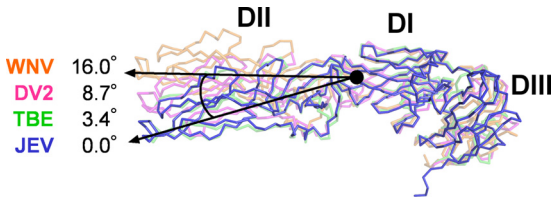

FIG 3 Comparison of E protein DI-DII hinge angles. The DI-DII hinge angle of JEV E is most similar to that of TBEV E. Various crystal structures of E were superimposed onto DI of JEV E, and the relative angle between DI and DII was determined using Dyndom. Proteins are colored according to the virus of origin, and the numbers on the left indicate the difference in angle between DI and DII of each E protein and JEV E. The DV3 E protein was omitted for clarity and because it varies by <1° from that of DV2 E.

ically significant interfaces. Interestingly, in all E structures the S_c of the fusion loop pocket was greater than the DII-DII region, suggesting that the precise fit of this peptide is of functional importance.

DI-DII hinge angle. The angle between DI and DII varies substantially throughout the viral life cycle. The relative change in hinge angle between JEV E and that all other available prefusion E protein structures was calculated by using Dyndom by individually superimposing JEV DI and DII onto those of WNV, DV2, DV3, and TBEV E proteins (Fig. 3) (19). The most closely related E protein, that of WNV (~75% identity), exhibited the largest difference at 16.0°, but this structure is monomeric and likely represents a prefusion conformation or intermediate that occurs during the trimer transition. Of the remaining E proteins, the JEV hinge most closely resembled that of TBEV, with a difference of only 3.4°. This was surprising since the two viruses are only 38% identical and JEV E has only ca. 50% of the buried surface area relative to TBEV E. The differences in hinge for DV2 and DV3 E were found to be 8.7° and 9.6°, respectively. Although E molecules require flexibility to drive structural changes essential for infection, it appears they also adjust to accommodate species-specific dimer arrangements.

Structural contributions to the interface. Several loops of the JEV E dimer subunits are devoid of contacts present in those of DV2, DV3, and TBEV (Fig. 4). Three of these segments are specific to DV2 and DV3 E proteins. The first links strands B_o and C_o of DI and the second is the "k-l" loop of DII (Fig. 4A). In the DV2 and DV3 E structures, these peptides stretch across the assembly to pack against the 'i-j' loop from DII of the opposing subunit (Fig. 4A). No residue in any of these regions contributes a dimer contact in JEV E and its k-l loop actually angles up and away from the interface, in stark contrast to the conformation in DV2 E (Fig. 4C). TBEV E, on the other hand, lacks the contacts found in the DV E proteins but possesses a 6-amino-acid insertion between the f and g strands of DII (Fig. 4B). Five of these six residues were identified as contacts in the TBEV E dimer. This insertion lies atop the "b" and "j" strands of the antiparallel proteins, so while TBEV has a similar hinge angle to that of JEV, it buries additional surface area via this insertion. Sequence alignments of these regions of E proteins with known structures highlight their respective dimer contacts (Fig. 4D).

JEV E protein stoichiometry. To assess the oligomeric state of the JEV E protein, we utilized multi-angle light scattering. This technique directly determines absolute molecular weight from intrinsic scattering properties of proteins, so it is advantageous over methods such as dynamic light scattering or SEC that extrapolate from hydrodynamic radius alone. Purified JEV E was loaded onto an SEC column at a concentration of 20 μM, and the refractive index change and multiangle light scattering (MALS) were observed over the elution profile. JEV E eluted as a single peak with an experimentally determined molecular mass of 45.3 kDa (Fig.

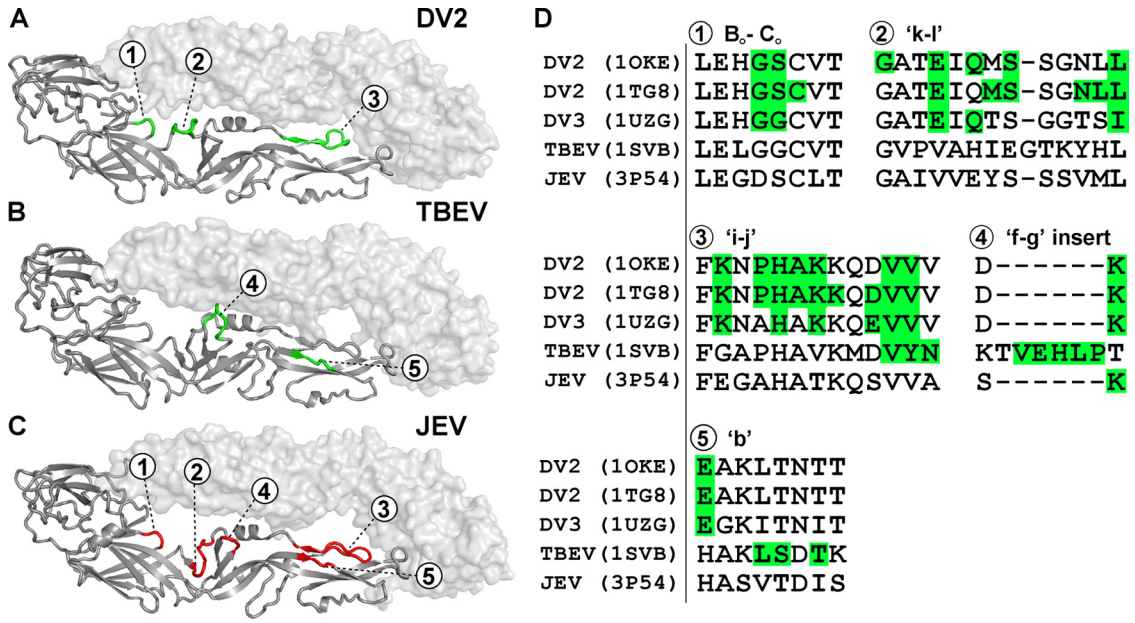

FIG 4 Dimeric contact residues in E proteins from DV, TBEV, and JEV serocomplexes. Multiple loops of DI and DII have dimer contacts in TBEV and DV E that are lacking in JEV E. Loops colored green contribute to dimer contacts in the DV (A) and TBEV (B) E proteins but not in JEV E protein. (C) The equivalent loops are colored red in the JEV E structure. (D) The sequences corresponding to the numbered loops are aligned for all known dimeric E protein structures, with dimer contact residues highlighted in green. The parent virus of the E protein and its PDB ID are shown to the left of each sequence.

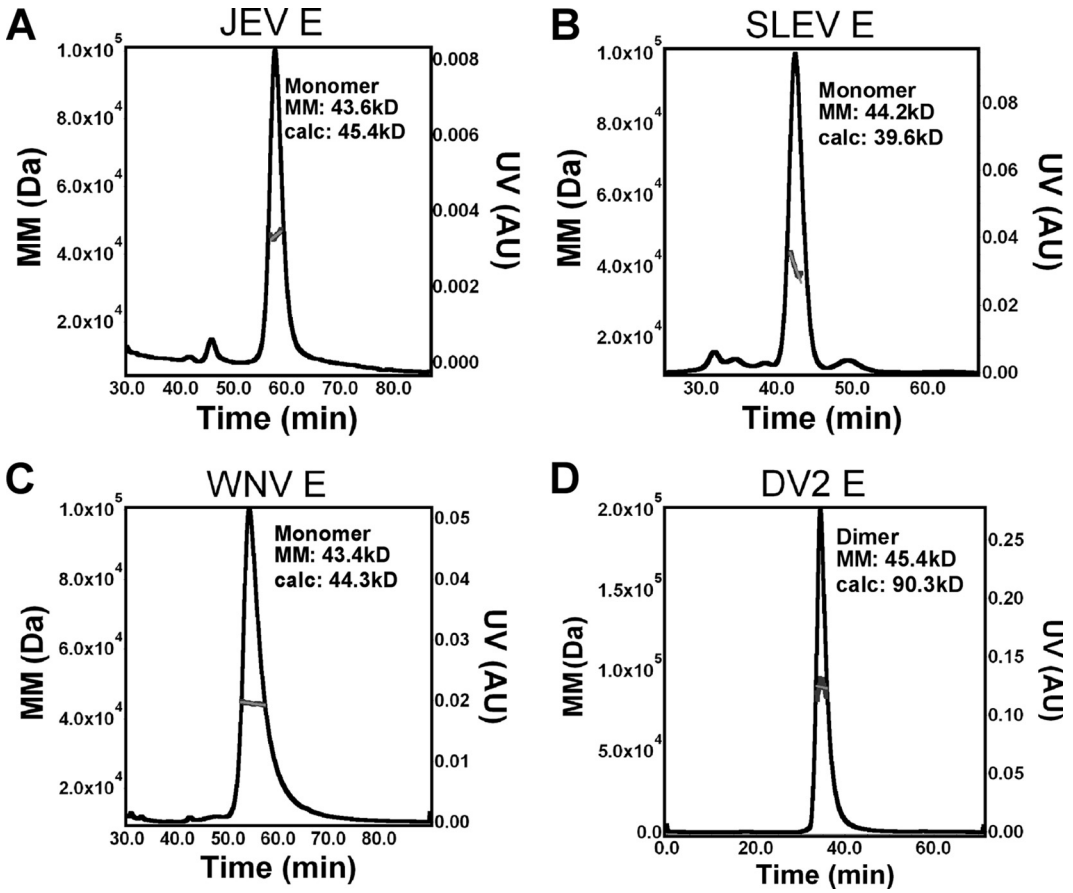

FIG 5 Multi-angle light scattering evaluation of E protein solution oligomeric state. E proteins from viruses of the JEV E serocomplex favor a monomeric solution state. Multi-angle light scattering was utilized to calculate the solution molecular mass (MM) of JEV E (A), SLEV E (B), WNV E (C) and DV2 E (D) over their elution profile on a S200 sizing column. JEV E, SLEV E, and WNV E had molecular masses corresponding to that of monomers, whereas DV2 E was that of a dimer. The UV absorbance trace is colored black, molar mass calculation in blue and fitted molar mass in red.

5A). JEV E has a predicted molecular mass of 43.6 kDa, so while the soluble JEV E ectodomain packed as a crystallographic dimer, our observations demonstrate that it is predominantly monomeric in solution. The molecular masses of E proteins from WNV and SLEV were also determined in the same fashion. WNV E yielded a mass of 44.3 kDa (predicted, 43.4 kDa) and SLEV yielded a mass of 39.6 kDa (predicted, 44.2 kDa), both of which correspond to that of a monomer (Fig. 5B and C). It has been previously reported that DV2, DV3, and TBEV were solution dimers, so we evaluated the oligomeric state of DV2 E to validate our assay (Fig. 5D) (38, 39, 52, 65). Insect cell expressed DV2 E was utilized in these experiments since we have not been able to successfully refold DV E proteins from bacterial inclusion bodies. However, previous studies have indicated that insect cell expressed WNV E is monomeric in solution, suggesting that the single N-linked glycan does not play a significant role in the oligomeric state of the soluble ectodomain (47). DV2 E indeed had a molecular mass of 90.3 kDa (predicted, 45.4 kDa) corresponding to that of a dimer. Thus, E ectodomains from the JEV antigenic complex (JEV, SLEV, and WNV) were all found to have monomeric molecular masses (Fig. 5A to C), whereas the DV2 E protein exists predominantly as a dimer in solution (Fig. 5D). The propensity of JEV E to remain as a solution monomer is consistent with the smaller dimer interface we observed relative to DV2 E.

Superimposition onto the DV cryo-EM model. Determination of the cryo-electron microscopy (cryo-EM) structures of DV and WNV revealed a framework of E protein dimers within the context of virion icosahedral symmetry (31, 41). In order to evaluate whether the domain organization of our JEV E structure could serve as a suitable atomic model within the context of an icosahedral virion, we superimposed unmodified monomer subunits onto the main chain coordinates of DV2 E from the cryo-EM reconstruction. The JEV E crystal structure adequately superimposes onto the arrangement with the only clash between main chains occurring in the b-c and h-i loops at the lateral edge of DII at the 2-fold axis (Fig. 6A). This was unexpected given that generation of an icosahedral virion with other structures required the disassembly of E into domains and rigid body refinement to prevent clashes, suggesting the domain organization found in our JEV E crystal structure could reasonably represent that of its native virion (65). Next, a general analysis of the dimer interface of DV2, DV3, JEV, and TBEV E crystal structures was performed to compare the dimer interfaces of these structures with those produced by superimposition onto the DV2 model. The mock JEV dimers generated were calculated to bury 469 Å^2 of surface area, yielding a difference of 364 Å^2 compared to the crystallographic dimer (Fig. 6C). The buried dimer surface areas of other E dimers generated in the same fashion were 404 Å^2 for DV2 (PDB 1TG8), 424

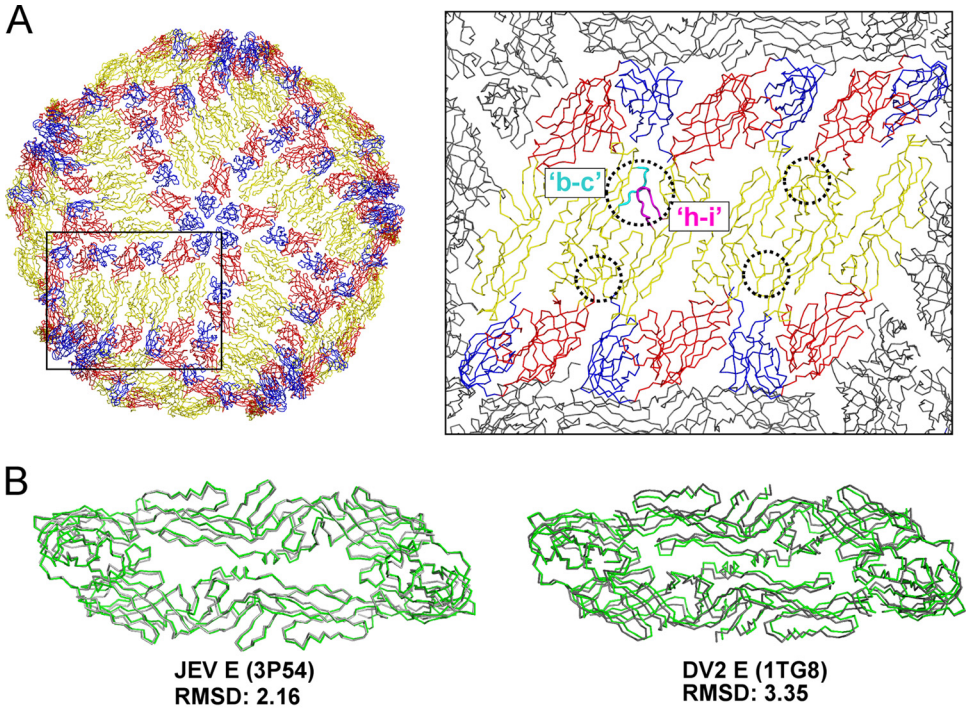

C

	Buried surface area (crystal) Å^2	Buried surface area (cryoEM) Å^2	RMSD crystal dimer: cryoEM dimer Å
JEV E	843	469	2.16
TBEV E	1496	975	2.43
DV2 E	1703	404	3.35
DV3 E	1593	424	2.83

FIG 6 Comparison of E protein crystal structures to DV2 cryo-EM model. (A) Superimposition of the unmodified JEV E crystal structure onto the DV2 cryo-EM coordinates generates an effective model for the JEV virion. JEV E monomers were superimposed onto E proteins from the DV2 cryo-EM reconstruction. The enlarged window of E proteins at the 2-fold axis shows the only clashing main-chain loops, "b-c" and "h-i", in cyan and magenta, respectively. (B) JEV E and DV2 E crystal structure backbones (green) are overlaid onto artificially generated dimers created by superimposing monomers from the crystal structure onto Dengue E dimers of the cryo-EM model (gray). (C) The table describes the buried surface areas from the crystal structures, the cryo-EM model dimers and the RMSD obtained by aligning the crystal structure dimers onto the cryo-EM models.

Å^2 for DV3 (PDB 1UZG), and 975 Å^2 for TBEV (PDB 1SVB), representing substantially greater differences in buried surface area (BSA) compared to those of their respective crystal structures (Fig. 6C). In addition, aligning entire dimers from the crystal structures onto the corresponding superimposed cryo-EM dimers yielded RMSDs of 2.16 Å for JEV E, 2.43 Å for TBEV E, 3.35 Å for DV2 E, and 2.83 Å for DV3 E (Fig. 6B). In conjunction with the BSA calculations, this RMSD findings suggest that the JEV E structure provides an effective model for its assembly in the mature virion.

Localization of histidines. It has been suggested that protonation of histidines at acidic pH plays an important role in the flavivirus life cycle, especially during the structural transition that leads to membrane fusion. Proposed functions of these residues include homodimer dissociation, conformational changes of DIII and trimerization (16). Mutation of broadly conserved H^{323} of TBEV E was shown to decrease infectivity, but substitution of each of the individual histidines of WNV E did not have an effect, suggesting that for some viruses they may act in concert (16, 44). In JEV E, most are found at the dimer interface, DI-DIII and DI-DII hinges, locations relevant to their proposed roles. Others, however, are situated along the lateral ridge on DII and DIII. Four histidines—His^{144}, His^{246}, His^{284}, and His^{319}—are entirely conserved in flaviviruses and found at the dimer interface and interdomain hinges. Three others—His^{81}, His^{395}, and His^{397}—are poorly represented in most flaviviruses but conserved within the JEV serocomplex and positioned at surfaces distal to the dimer interface (Fig. 7). Protonation of the three serocomplex-specific histidines at this lateral edge would likely have an effect on the quaternary arrangement of adjacent subunits based on the modeling of JEV E into the DV cryo-EM reconstruction. The conservation at these positions may provide additional energy to stabilize JEV E within the icosahedral framework at neutral pH, possibly compensating for lost contributions at the dimer interface. At acidic pH, the protonation of these His residues outside the dimer interface may be an important mechanism for the regulation of viral uncoating.

Neutralizing epitopes. Mapping of antibodies onto the three-dimensional structures of the WNV and DV E proteins has revealed the localization of dominant neutralizing epitopes (49).

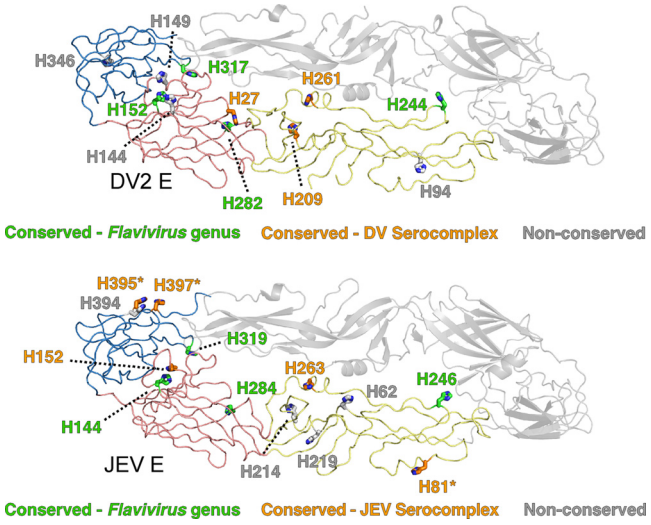

FIG 7 Conservation and localization of histidines of E proteins from the JEV and DV serocomplexes. Histidines on the lateral edge of DII and DIII are poorly represented in flaviviruses but conserved in the JEV serocomplex. Histidines of the DV2 E and JEV E proteins are shown in stick representation on one dimer subunit and labeled with their residue number for the given virus. Those colored green represent those conserved in all flaviviruses, those colored orange are conserved in only the DV2 (top) or JEV serocomplex (bottom), and those colored gray are not broadly conserved. Histidines fully conserved in the JEV serocomplex but not in other flaviviruses are found on the outer edge of the dimer and marked with an asterisk.

Antibodies that neutralize flaviviruses localize to specific regions of the protein that span all three E protein domains, with the observation that many of the most potently neutralizing monoclonal antibodies recognize the lateral ridge and "A" strand of DIII (6, 14, 46, 49, 54, 59). Several studies have identified individual residues essential to recognition of JEV by neutralizing antibodies A3, B2, E3, NARMA3, 503, 4G2, and E3.3 (9, 17, 28, 40, 62, 63). We have compiled and highlighted these residues on the crystal structure and mature virion model of JEV E. These fall into four distinct regions: the DI-DII hinge, DI lateral ridge, and DIII lateral ridge epitopes, which are exposed in the cryo-EM structure, and the buried fusion loop (Fig. 8A) (48, 49). Antibodies B2 (I^{126}), NARMA3 (Q^{52}), and 503 (Q^{52}, I^{126}, K^{136}, and S^{275}) all bind exposed residues in the DI-DII hinge region (Fig. 8C). Antibody A3 (K^{179}) maps to the DI lateral ridge (Fig. 8D), and antibodies E3 (G^{302}) and E3.3 (I^{337}, F^{360}, R^{387}) recognize the DIII lateral ridge (Fig. 8E). Broadly cross-reactive antibody 4G2 has been shown to weakly neutralize JEV and interacts with residues 104, 106, and 107 at the tip of the fusion loop (Fig. 8B). The DI-DII hinge and DI and DIII lateral ridge epitopes are all largely exposed on the JEV mature virion, the exception being epitopes located where DIII packs at the inner 5-fold axis. It has been previously reported that antibodies binding WNV E at a similar epitope are also inaccessible (24). The fusion loop epitope is commonly recognized by broadly cross-reactive antibodies and is partially buried in the JEV E model virion. This epitope is likely only transiently exposed due to motions of E proteins in the virion or in particles that contain E in the immature conformation.

DISCUSSION

The structure of the JEV E ectodomain was determined to identify unique characteristics of this important pathogen. A notable feature of our high-resolution structure is the unusual dimeric interface of the E subunits. Measurements of homodimer buried surface area, shape complementarity, hydrogen bonds, and salt bridges each indicate a less substantial interface relative to those of TBEV, DV2, and DV3. We determined the oligomeric state of JEV, SLEV, and WNV E proteins and found that all were solution monomers consistent with our JEV structure, as well as two independent crystal structures of monomeric WNV E (23, 47). While JEV serocomplex members were produced with a bacterial expression system, the conserved disulfide bond connectivity observed in JEV E, as well as the propensity of the related SLEV E protein to crystallize as a trimer at low pH (unpublished data), indicates that these molecules are properly folded and functional. Our results suggest that flavivirus evolution has modulated the E homodimer interface and dimeric affinity, which may substantially affect recognition by antibodies and cellular receptors.

Cryo-EM structures of mature WNV and DV have revealed a tightly packed "herringbone" arrangement of E proteins in which the dimer interface and lateral ridges of all three domains support a stable icosahedral framework (31, 41). E protein homodimerization has been thought to be a primary building block of the mature flavivirus virion, so it was surprising to find that JEV E and related serocomplex proteins were solution monomers. An explanation for the disparate dimer properties of the JEV envelope could be that it relies upon quaternary contacts among dimers rather than the dimer interface *per se* as principal load-bearing points in the viral chassis. Preliminary infectivity experiments indicate that despite its small dimer interface JEV exhibits greater thermostability than DV2 (J. D. Brien and M. S. Diamond, unpublished data). These results suggest virions are likely stabilized by a complex network of quaternary interactions outside of the dimer interface. Consistent with this hypothesis is the location of the JEV serocomplex's uniquely conserved histidines at the outer edges of the E protein, where quaternary contacts would be made with other E dimer rafts. While mutation of individual histidine residues does not have a significant effect on WNV infectivity, it has been proposed that protonation of multiple histidines in concert may drive E homodimer dissociation as an essential step in the series of conformational changes that lead to membrane fusion (16, 44). Strikingly, three of nine histidines conserved in the JEV serocomplex (Fig. 7) are found on the lateral edge of E rather than at hinge regions or the dimer interface, suggesting that these viruses may utilize pH to regulate structural transitions by breaking nondimer interfaces.

Analysis of contact residues across E proteins revealed specific structural differences between the JEV homodimer and that of DV or TBEV. Two DII loops, "k-l" of DV2/3 and "f-g" of TBEV, make contributions to the interface that are entirely absent in JEV E. The k-l loop angles forward in one structure of DV2 E (1OKE) and creates a pocket that the hydrophobic ligand *n*-octyl-β-D-glucoside was observed to bind crystallographically (38). In the JEV E structure, this loop is splayed away from the interface but opens a channel ~15 Å in diameter where these contacts would be made in DV2 E (Fig. 2). These channels are large enough to accommodate the insertion of a host ligand, raising the possibility that their presence or absence could influence viral tropism by modulating receptor interaction. Alternatively, the major contributor of E dimer contacts present in TBEV but not JEV is the f-g loop of DII. In TBEV, the f-g loop contains a 6-amino-acid insertion that positions itself atop the "b" and "j" strands from the

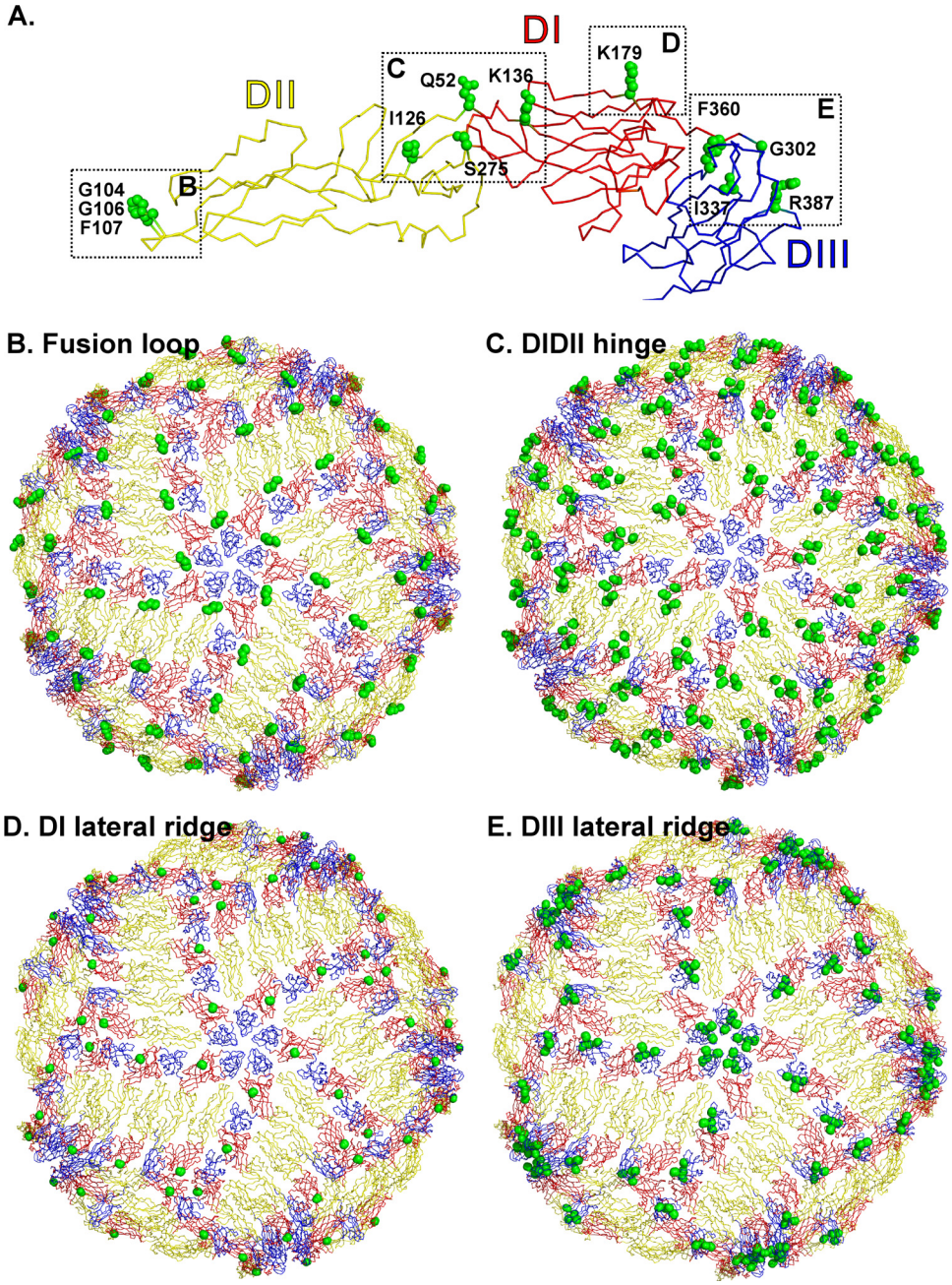

FIG 8 Mapping of neutralizing epitopes onto the JEV E protein and reconstructed virion. JEV E neutralizing epitopes are found at the DI-DII hinge, DI lateral ridge, DIII lateral ridge, and fusion loop. (A) Side chains of residues critical for binding by previously identified JEV neutralizing antibodies are colored green and in spherical representation. (B) 4G2 (G^{104}, G^{106}, and L^{107}) maps to the fusion loop. (C) B2 (I^{126}), NARMA3 (Q^{52}), and 503 (Q^{52}, I^{126}, K^{136}, and S^{275}) map to the DI-DII hinge. (D) A3 (K^{179}) maps to the DI lateral ridge. (E) E3 (G^{302}) and E3.3 (I^{337}, F^{360}, and R^{387}) map to the DIII lateral ridge. The regions described above have also been mapped onto the model of the JEV virion to reveal their arrangement and accessibility in the icosahedral assembly.

opposing DII and appears to latch the subunits together. Other TBEV E serocomplex members, Powassan virus and Langat virus, also share this insertion. Notably, a histidine residue H^{208} is conserved at the apex of the loop so protonation at low pH could provide energy to repel the molecules apart.

While our comparison of E proteins has highlighted differences between the crystal structures, serological data suggest that E may adopt a continuum of distinct conformations on the surface of the virion. Structural proteins from flaviviruses, picornaviruses, nodaviruses, and rhinoviruses are all believed to exhibit flexibility within their icosahedral organization (4, 13, 14, 33, 34). Evidence that has arisen from the study of both DIII and fusion loop-specific neutralizing antibodies strongly suggests that the cage of flavivirus E proteins ratchet through conformations specific to the virus that encodes them. It has been reported that high-temperature preincubation of DV with an anti-DIII Fab resulted in an unusual, distorted cryo-EM structure in which E was locked into a previously unobserved icosahedral assembly (34). The an-

tibody recognizes an epitope of DIII that is partially masked in mature virions, and yet the Fab managed to bind the virion and capture this unusual conformation. The WNV-specific antibody E16, on the other hand, binds a similar epitope and does not cause any significant changes in the mature arrangement upon binding (46). The range of motion of E proteins within a mature virion could thus be influenced by the packing of the dimer. Another class of antibodies bind the fusion loop epitope that is buried in the cryo-EM model of the mature virus particle, implying that it must be at least transiently exposed during its life cycle (9, 49). Unexpectedly, many of these fusion loop antibodies are broadly cross-reactive but do not cross-neutralize. JEV and TBEV, in particular, were found to have a poor correlation between the antibody affinity for their recombinant E proteins and neutralization titer, strongly suggesting that exposure of this conserved epitope differs from one viral species to the next (58). One fusion-loop antibody, E53, has even been reported to preferentially recognize the E protein spikes that occur in immature virions (7). Indeed, partially mature virions would be predicted to have the propensity for unique assembly based on the number and location of uncleaved prM (7, 22, 53). The resulting permuted distortions of the E protein network likely results in arrangements not represented by the icosahedral geometry of reported cryo-EM models.

It is becoming increasingly clear that the distinct arrangement of flavivirus E protein subunits can affect antibody recognition and neutralization. Recent evidence has described a neutralizing Fab with a paratope that cross-links two independent E proteins on the surface of the virion (25). Although this antibody bound icosahedral axes outside of the dimer interface, its discovery supports the notion that specific organization of JEV, DV, and TBEV E proteins can influence molecular recognition events of the virion. Additional factors that may influence E presentation on the particle surface are the transmembrane and stem-loop regions not present in the crystal structures (26). However, their influence does not oppose the hypothesis that quaternary organization or flexibility could be distinct for individual flaviviruses.

In conclusion, the structure of the JEV E ectodomain has revealed a uniquely small dimer interface that may play a role in flavivirus stabilization, immunorecognition and pathogenesis. Features of the protein, including its monomeric solution state, relatively low buried surface area, and location of serocomplex-conserved histidines, suggest that it is representative of its native state in the virion. Superimposition of JEV E onto the DV cryo-EM structure of the mature virion results in only a single clash and did not require the separation of domains to effectively reconstruct a JEV particle. This model also highlights the residues recognized by several classes of neutralizing antibody, indicating both surface exposed and buried epitopes. Since both clearance and enhancement of flavivirus infections strongly depend on antibody recognition of complex E protein epitopes, continued evaluation of intricate structural features of these proteins is essential to the design of future therapeutics and vaccines.

ACKNOWLEDGMENTS

This study was supported in part by the Center for Structural Genomics of Infectious Diseases (contract HHSN272200700058C).

We thank Mike Diamond, James Brien, Kelly Smith, Melissa Barrow, and Kyle Austin for helpful discussions and experimental suggestions.

REFERENCES

1. **Adams PD, et al.** 2002. PHENIX: building new software for automated crystallographic structure determination. Acta Crystallogr. D Biol. Crystallogr. **58**:1948–1954.
2. **Allison SL, et al.** 1995. Oligomeric rearrangement of tick-borne encephalitis virus envelope proteins induced by an acidic pH. J. Virol. **69**:695–700.
3. **Allison SL, Schalich J, Stiasny K, Mandl CW, Heinz FX.** 2001. Mutational evidence for an internal fusion peptide in flavivirus envelope protein E. J. Virol. **75**:4268–4275.
4. **Bothner B, Dong XF, Bibbs L, Johnson JE, Siuzdak G.** 1998. Evidence of viral capsid dynamics using limited proteolysis and mass spectrometry. J. Biol. Chem. **273**:673–676.
5. **Bressanelli S, et al.** 2004. Structure of a flavivirus envelope glycoprotein in its low-pH-induced membrane fusion conformation. EMBO J. **23**:728–738.
6. **Brien JD, et al.** 2010. Genotype-specific neutralization and protection by antibodies against dengue virus type 3. J. Virol. **84**:10630–10643.
7. **Cherrier MV, et al.** 2009. Structural basis for the preferential recognition of immature flaviviruses by a fusion-loop antibody. EMBO J. **28**:3269–3276.
8. **Chu JJ-H, Ng M-L.** 2004. Interaction of West Nile virus with $\alpha v\beta 3$ integrin mediates virus entry into cells. J. Biol. Chem. **279**:54533–54541.
9. **Crill WD, Chang G-JJ.** 2004. Localization and characterization of flavivirus envelope glycoprotein cross-reactive epitopes. J. Virol. **78**:13975–13986.
10. **Davis CW, et al.** 2006. The location of asparagine-linked glycans on West Nile virions controls their interactions with CD209 (dendritic cell-specific ICAM-3 grabbing nonintegrin). J. Biol. Chem. **281**:37183–37194.
11. **Davis CW, et al.** 2006. West Nile virus discriminates between DC-SIGN and DC-SIGNR for cellular attachment and infection. J. Virol. **80**:1290–1301.
12. **De Madrid AT, Porterfield JS.** 1974. The flaviviruses (group B arboviruses): a cross-neutralization study. J. Gen. Virol. **23**:91–96.
13. **Delaet I, Boeyé A.** 1994. Capsid destabilization is required for antibody-mediated disruption of poliovirus. J. Gen. Virol. **75**(Pt 3):581–587.
14. **Delaet I, Boeyé A.** 1993. Monoclonal antibodies that disrupt poliovirus only at fever temperatures. J. Virol. **67**:5299–5302.
15. **Elshuber S, Allison SL, Heinz FX, Mandl CW.** 2003. Cleavage of protein prM is necessary for infection of BHK-21 cells by tick-borne encephalitis virus. J. Gen. Virol. **84**:183–191.
16. **Fritz R, Stiasny K, Heinz FX.** 2008. Identification of specific histidines as pH sensors in flavivirus membrane fusion. J. Cell Biol. **183**:353–361.
17. **Goncalvez AP, et al.** 2008. Humanized monoclonal antibodies derived from chimpanzee Fabs protect against Japanese encephalitis virus in vitro and in vivo. J. Virol. **82**:7009–7021.
18. **Hanna SL, et al.** 2005. N-linked glycosylation of West Nile virus envelope proteins influences particle assembly and infectivity. J. Virol. **79**:13262–13274.
19. **Hayward S, Berendsen HJ.** 1998. Systematic analysis of domain motions in proteins from conformational change: new results on citrate synthase and T4 lysozyme. Proteins **30**:144–154.
20. **He RT, et al.** 1995. Antibodies that block virus attachment to Vero cells are a major component of the human neutralizing antibody response against dengue virus type 2. J. Med. Virol. **45**:451–461.
21. **Huang CY-H, et al.** 2010. The dengue virus type 2 envelope protein fusion peptide is essential for membrane fusion. Virology **396**:305–315.
22. **Junjhon J, et al.** 2010. Influence of pr-M cleavage on the heterogeneity of extracellular dengue virus particles. J. Virol. **84**:8353–8358.
23. **Kanai R, et al.** 2006. Crystal Structure of West Nile virus envelope glycoprotein reveals viral surface epitopes. J. Virol. **80**:11000–11008.
24. **Kaufmann B, et al.** 2006. West Nile virus in complex with the Fab fragment of a neutralizing monoclonal antibody. Proc. Natl. Acad. Sci. **103**:12400–12404.
25. **Kaufmann B, et al.** 2010. Neutralization of West Nile virus by cross-linking of its surface proteins with Fab fragments of the human monoclonal antibody CR4354. Proc. Natl. Acad. Sci. U. S. A. **107**:18950–18955.
26. **Kiermayr S, Stiasny K, Heinz FX.** 2009. Impact of quaternary organization on the antigenic structure of the tick-borne encephalitis virus envelope glycoprotein E. J. Virol. **83**:8482–8491.
27. **Kleywegt GJ, et al.** 2004. The Uppsala electron-density server. Acta Crystallogr. D Biol. Crystallogr. **60**:2240–2249.

28. **Kobayashi Y, Hasegawa H, Yamauchi T.** 1985. Studies on the antigenic structure of Japanese encephalitis virus using monoclonal antibodies. Microbiol. Immunol. **29**:1069–1082.
29. **Konno J, Endo K, Agatsuma H, Ishida N.** 1966. Cyclic outbreaks of Japanese encephalitis among pigs and humans. Am. J. Epidemiol. **84**:292–300.
30. **Krissinel E, Henrick K.** 2007. Inference of macromolecular assemblies from crystalline state. J. Mol. Biol. **372**:774–797.
31. **Kuhn RJ, et al.** 2002. Structure of dengue virus: implications for flavivirus organization, maturation, and fusion. Cell **108**:717–725.
32. **Lee JW-M, Chu JJ-H, Ng M-L.** 2006. Quantifying the specific binding between West Nile virus envelope domain III protein and the cellular receptor alphaVbeta3 integrin. J. Biol. Chem. **281**:1352–1360.
33. **Lewis JK, Bothner B, Smith TJ, Siuzdak G.** 1998. Antiviral agent blocks breathing of the common cold virus. Proc. Natl. Acad. Sci. U. S. A. **95**: 6774–6778.
34. **Lok S-M, et al.** 2008. Binding of a neutralizing antibody to dengue virus alters the arrangement of surface glycoproteins. Nat. Struct. Mol. Biol. **15**:312–317.
35. **Merritt EA, Painter J.** TLSMD web server for the generation of multi-group TLS models. J. Appl. Crystallogr. **39**:109–111.
36. **Minor W, Otwinowski Z.** 1997. Processing of X-ray diffraction data collected in oscillation mode. Methods Enzymol. **276**:307–326.
37. **Modis Y, Ogata S, Clements D, Harrison SC.** 2004. Structure of the dengue virus envelope protein after membrane fusion. Nature **427**:313–319.
38. **Modis Y, Ogata S, Clements D, Harrison SC.** 2003. A ligand-binding pocket in the dengue virus envelope glycoprotein. Proc. Natl. Acad. Sci. U. S. A. **100**:6986–6991.
39. **Modis Y, Ogata S, Clements D, Harrison SC.** 2005. Variable surface epitopes in the crystal structure of dengue virus type 3 envelope glycoprotein. J. Virol. **79**:1223–1231.
40. **Morita K, et al.** 2001. Locus of a virus neutralization epitope on the Japanese encephalitis virus envelope protein determined by use of long PCR-based region-specific random mutagenesis. Virology **287**:417–426.
41. **Mukhopadhyay S, Kim B-S, Chipman PR, Rossmann MG, Kuhn RJ.** 2003. Structure of West Nile virus. Science **302**:248.
42. **Navarro-Sanchez E, et al.** 2003. Dendritic-cell-specific ICAM3-grabbing non-integrin is essential for the productive infection of human dendritic cells by mosquito-cell-derived dengue viruses. EMBO Rep. **4**:723–728.
43. **Nayak V, et al.** 2009. Crystal structure of dengue virus type 1 envelope protein in the postfusion conformation and its implications for membrane fusion. J. Virol. **83**:4338–4344.
44. **Nelson S, Poddar S, Lin T-Y, Pierson TC.** 2009. Protonation of individual histidine residues is not required for the pH-dependent entry of West Nile virus: evaluation of the "histidine switch" hypothesis. J. Virol. **83**: 12631–12635.
45. **Nothdurft HD, et al.** 1996. Adverse reactions to Japanese encephalitis vaccine in travelers. J. Infect. **32**:119–122.
46. **Nybakken GE, et al.** 2005. Structural basis of West Nile virus neutralization by a therapeutic antibody. Nature **437**:764–769.
47. **Nybakken GE, Nelson CA, Chen BR, Diamond MS, Fremont DH.** 2006. Crystal structure of the West Nile virus envelope glycoprotein. J. Virol. **80**:11467–11474.
48. **Oliphant T, et al.** 2005. Development of a humanized monoclonal antibody with therapeutic potential against West Nile virus. Nat. Med. **11**: 522–530.
49. **Oliphant T, et al.** 2006. Antibody recognition and neutralization determinants on domains I and II of West Nile virus envelope protein. J. Virol. **80**:12149–12159.
50. **Painter J, Merritt EA.** 2006. Optimal description of a protein structure in terms of multiple groups undergoing TLS motion. Acta Crystallogr. D Biol. Crystallogr. **62**:439–450.
51. **Plesner, A-SH.** 1998. Neurological complications to vaccination against Japanese encephalitis. Eur. J. Neurol. **5**:479–485.
52. **Rey FA, Heinz FX, Mandl C, Kunz C, Harrison SC.** 1995. The envelope glycoprotein from tick-borne encephalitis virus at 2 Å resolution. Nature **375**:291–298.
53. **Rodenhuis-Zybert IA, et al.** 2010. Immature dengue virus: a veiled pathogen? PLoS Pathog. **6**:e1000718.
54. **Sánchez MD, et al.** 2005. Characterization of neutralizing antibodies to West Nile virus. Virology **336**:70–82.
55. **Schiøler KL, Samuel M, Wai KL.** 2007. Vaccines for preventing Japanese encephalitis. Cochrane Database Syst. Rev. CD004263.
56. **Solomon T, Vaughn DW.** 2002. Pathogenesis and clinical features of Japanese encephalitis and West Nile virus infections. Curr. Top. Microbiol. Immunol. **267**:171–194.
57. **Stadler K, Allison S, Schalich J, Heinz F.** 1997. Proteolytic activation of tick-borne encephalitis virus by furin. J. Virol. **71**:8475–8481.
58. **Stiasny K, Kiermayr S, Holzmann H, Heinz FX.** 2006. Cryptic properties of a cluster of dominant flavivirus cross-reactive antigenic sites. J. Virol. **80**:9557–9568.
59. **Sultana H, et al.** 2009. Fusion loop peptide of the West Nile virus envelope protein is essential for pathogenesis and is recognized by a therapeutic cross-reactive human monoclonal antibody. J. Immunol. **183**:650–660.
60. **Takahashi H, Pool V, Tsai TF, Chen RT.** 2000. Adverse events after Japanese encephalitis vaccination: review of post-marketing surveillance data from Japan and the United States. Vaccine **18**:2963–2969.
61. **Thompson BS, et al.** 2009. A therapeutic antibody against west nile virus neutralizes infection by blocking fusion within endosomes. PLoS Pathog. **5**:e1000453.
62. **Vogt MR, et al.** 2009. Human monoclonal antibodies against West Nile virus induced by natural infection neutralize at a postattachment step. J. Virol. **83**:6494–6507.
63. **Wu K-P, et al.** 2003. Structural basis of a flavivirus recognized by its neutralizing antibody: solution structure of the domain III of the Japanese encephalitis virus envelope protein. J. Biol. Chem. **278**:46007–46013.
64. **Yu I-M, et al.** 2008. Structure of the immature dengue virus at low pH primes proteolytic maturation. Science **319**:1834–1837.
65. **Zhang Y, et al.** 2004. Conformational changes of the flavivirus E glycoprotein. Structure **12**:1607–1618.